



ELSEVIER

Journal of Electron Spectroscopy and Related Phenomena 122 (2002) 239–249

JOURNAL OF  
ELECTRON SPECTROSCOPY  
and Related Phenomena

www.elsevier.com/locate/elspec

# Cathodoluminescence of small silver particles on $\text{Al}_2\text{O}_3/\text{NiAl}$ (110)

W. Drachsel, M. Adelt, N. Nilius, H.-J. Freund\*

*Fritz-Haber-Institut der Max-Planck-Gesellschaft, Faradayweg 4-6, D14195 Berlin, Germany*

Received 21 May 2001; received in revised form 8 October 2001; accepted 11 October 2001

## Abstract

Cathodoluminescence experiments have been performed on silver clusters, which were grown on well characterized  $\text{Al}_2\text{O}_3$  films supported on (110) NiAl crystals. Cluster size and shape were varied via Ag deposition at different temperatures and annealing the samples afterwards. At an electron energy of 50 eV photon emission was observed at the (1,0) plasmon resonance, which was centered at 3.7 eV for a mean size particle at 10 nm. The blue shift of  $\sim 200$  meV is interpreted by the oblate shape of the particle, as also indicated by the position of the (weak) emission for the (1,1) plasmon. The underlying NiAl exerts minor influence on the plasmon resonance, as the induced image dipole does not couple to the plasmon because of its phase shift of roughly  $90^\circ$ . © 2002 Elsevier Science B.V. All rights reserved.

*Keywords:* Cathodoluminescence; Ag cluster; Alumina film; Mie plasmon; Blue shift

## 1. Introduction

Light absorption by excitation of surface plasmon resonances in silver and gold nanoparticles has been a well-known phenomenon for very long, and since the pioneering work by Mie [1] it is also theoretically well understood within the framework of classical electrodynamics. These Mie resonances were later identified as plasmon-polaritons [2], i.e. collective oscillations of the conduction electrons driven by the incident electromagnetic wave. This field of research still attracts considerable interest for both fundamental (collective phenomena) [3] and practical reasons (optical filters) [4].

Plasmon oscillations of silver clusters in the gas phase [5] or embedded in a solid matrix [6] and also

supported on dielectric substrates [7] are well investigated by UV–Vis absorption spectroscopy [2]. These investigations have given deep insight into the optical properties of the studied nanoparticles [8], and the fundamental question of how cluster shape and size or the dielectric as well as the chemical environment influence the resonance position and width is still under discussion. However, due to the lack of electrical conductivity of an extended dielectric support, the information on the morphology of these systems is limited to AFM studies [9] or TEM and related microscopies [10] after appropriate preparation of the sample. From this point of view the application of oxide films on a metal substrate supporting the metal nanocrystals overcomes this limitation and, in principal, opens the way to apply a vast arsenal of surface science techniques for additional studies of structural and electronic details. In fact, this concept of an oxide support is favoured in basic research as a model system for the study of

\*Corresponding author. Tel.: +49-308-413-4100; fax: +49-308-413-4101.

E-mail address: freund@fhi-berlin.mpg.de (H.-J. Freund).

catalytic performance [11]. The chemical inertness of the oxide surface or, in other words, the lack of wetting promotes the growth of 3-dimensional metal aggregates on top. However, concerning their optical properties an electromagnetic interference with the metal substrate (in this case NiAl) beneath the  $\text{Al}_2\text{O}_3$  film is to be expected.

The commonly applied optical extinction spectroscopy probes the allowed electronic dipole transitions of the specimen investigated, but the deexcitation channels are not directly accessible by this method. The radiative deexcitation of the Mie plasmons in silver nanoparticles can be observed, if the plasmon polaritons of such deposited particles are excited by electron impact. The clusters then emit light. This behaviour of silver clusters deposited on well ordered alumina films has been recently examined for individual entities performing the excitation by electrons from an STM tip [12,13]. In this contribution we are concerned with the optical properties of an ensemble, by measuring the spectral photon yield during irradiation of the probe with low energy electrons from a distant source.

## 2. Experimental

The cathodoluminescence experiments have been carried out in an ultra-high vacuum system with a base pressure of  $9 \times 10^{-11}$  mbar; the chamber (Fig. 1)

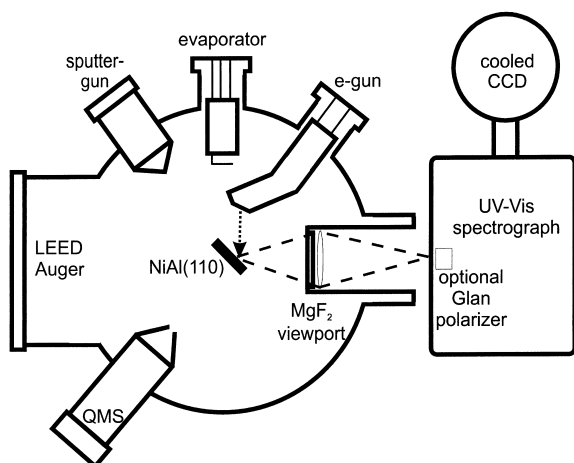


Fig. 1. Experimental set-up.

is equipped with an electron-beam evaporator, a low energy electron gun, a sputter source, a quadrupole residual gas analyzer and an LEED/Auger facility. The specimen was connected to a cool finger allowing cooling down to 30 K and heating up to 1300 K.

The (110) oriented NiAl crystal was cleaned by Ar sputtering at 650 K, by annealing at 1000 and flashing then to 1300 K. The alumina film was prepared by oxidation of the cleaned NiAl alloy surface at 500 K according to well-known recipes [14]. The formed alumina film has a  $\gamma\text{-Al}_2\text{O}_3$  (111)-like structure and a uniform thickness of 4–5 Å [15]. The surface structure was checked by LEED.

Silver was deposited on the film from an electron beam Ag evaporator. The deposition rate had been calibrated by measuring the flux of metal atoms by a quartz crystal balance. Because of the weak metal/oxide interaction silver grows in the Vollmer/Weber mode forming 3-dimensional particles. In order to vary the cluster size distribution the amount of deposited metal and the sample temperature was controlled during the nucleation process. Deposition at room temperature led to larger particles while formation at 90 K and even more at 30 K resulted in a higher density of smaller particles, that are more homogeneously distributed on the film although even at this temperature Ag tends to nucleate at defects [16]. Amounts of metal varied in the range of an effective thickness of 1 to 15 Å resulting in particle diameters of 5 to 12 nm as shown in the STM topographies in Fig. 2. In Fig. 2b the artefacts in the micrograph demonstrate the easy manipulation of the silver cluster by the STM tip. By including an  $\text{Ag}^+$  flux during deposition, the resulting sites yielded as nucleation centers for rather immovable Ag aggregates. The luminescence of the silver particles was recorded at the same sample temperature at which Ag was deposited, if not mentioned otherwise.

Light emission of the supported silver cluster was stimulated by electron impact from a low energy electron source. The used electron gun had a very low stray light emission and its design is described in detail in Ref. [17]. Typical energies used amounted from 20 to 50 eV, the currents at the probe ranged from 1 to 5  $\mu\text{A}$ . The electrons hit the specimen surface at oblique incidence of 45 degrees providing a spot diameter of 1 mm.

Below the probe a tungsten sheet covered with a

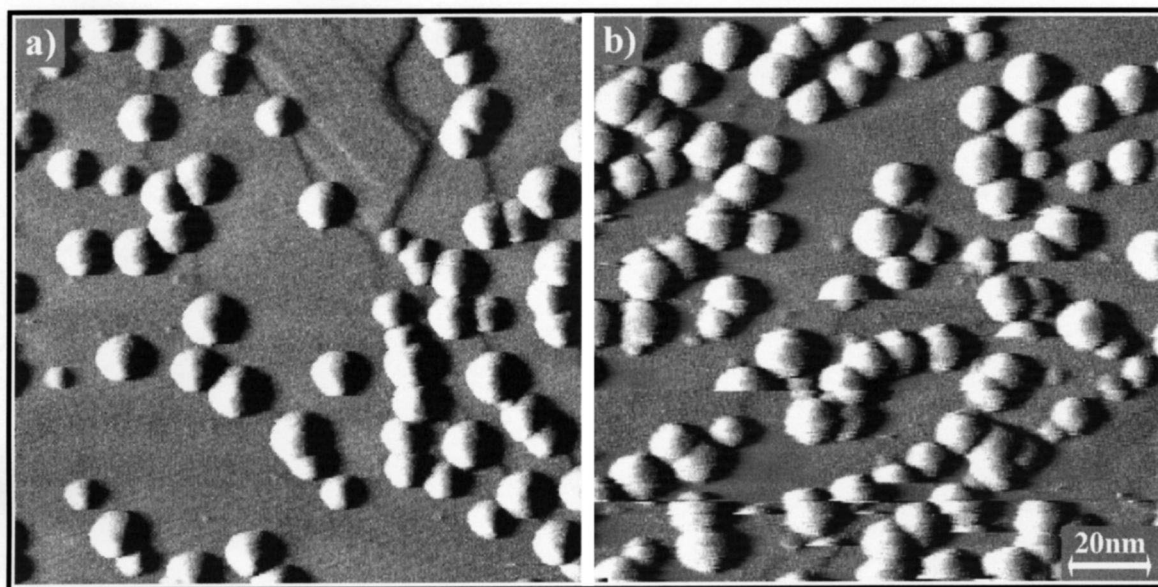


Fig. 2. STM micrograph of silver cluster on an  $\text{Al}_2\text{O}_3$  film, deposition at 300 K, CCT differential,  $138 \times 138 \text{ nm}^2$ , (a)  $U_{\text{tip}} = +1 \text{ V}$ , average thickness 2 Å; (b)  $U_{\text{tip}} = -2 \text{ V}$ , average thickness 5 Å.

$\text{CaWO}_4$  film was additionally mounted in order to calibrate the photosensitivity of the total system and to localize easily the position of the electron spot due to the high and well-characterized cathodoluminescence of this material [18].

The luminescence spectra of the supported Ag clusters were recorded with a UV–Vis spectrometer in connection with a liquid nitrogen-cooled CCD detector (Triax 180, Instruments S.A.) in the energy range of 1.2 to 6.2 eV using a 150 line grating with a resolution of 3 nm. A  $\text{MgF}_2$  lens focused the emitted light (collection angle 0.8 rad) from the sample onto the entrance slit of the monochromator, a polarisator could be inserted in the beam path additionally. Due to the low light intensity of the studied processes, integration time for quality spectra was 15 min. The estimated overall detection sensitivity of the spectroscopic configuration was  $10^{-8}$  counts recorded per one photon emitted into the semi sphere from the probe surface. The spectra were corrected for the spectral sensitivity of the CCD detector. As the spectrometer measures the intensity  $I(\lambda)$  per interval  $\Delta\lambda$ , the presented energy-dependent intensity  $I(\hbar\omega)$  is evaluated from the  $I(\lambda) \times \lambda^2$  conversion.

### 3. Results and discussion

#### 3.1. NiAl substrate

The clean NiAl substrate faintly emits light at a photon energy around 2.6 eV upon electron impact, unchanged by an alumina layer on it. This luminescence spectrum is shown in Fig. 3, a preferential polarization of the emitted photons was not observed. The same emission spectrum is also observed in the STM, when the tip is far above the NiAl surface and if a tip voltage of ca.  $-50 \text{ V}$  is applied [19].

The imaginary part  $\varepsilon_2$  of the dielectric function for the alloy NiAl [20] plotted for comparison in Fig. 3 gives rise to a maximum value at the same energy. However, at the second maximum in  $\varepsilon_2$  of 4.1 eV, no light emission is observed by both methods (Fig. 3). The interpretation of the luminescence in the framework of transition radiation or bremsstrahlung [21,22] is controversial. These concepts seem to be only adequate at electron impact energies in the kV-range as applied in TEM studies [21]. Several authors [23,24] assign the experimentally observed

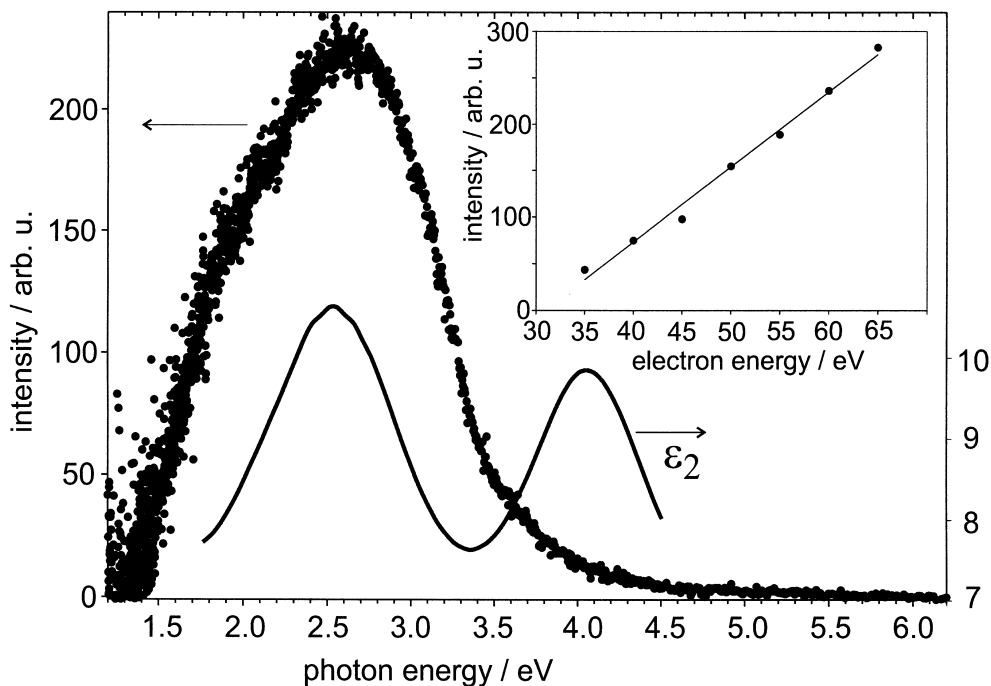


Fig. 3. Photon emission from NiAl. Luminescence spectrum at an electron energy of 50 eV. For comparison the imaginary part of the dielectric function  $\epsilon_2$  is included. The insert shows the luminescence intensity versus electron energy.

absorption at a photon energy of 2.5 eV for NiAl as a transition from the Fermi level to an unoccupied state above. In this case a rather high recombination rate is expected as the density of available electron holes is very high at the Fermi level, which explains the NiAl-luminescence band centered at this energy. The absorption at 4.2 eV is interpreted as an electronic excitation from 2.2 eV below to 2 eV above the Fermi level [24]. In this case the quenching of the holes and numerous competing transitions will prevent a radiative transition at this photon energy and will lead to the absence of the corresponding band in the emission spectrum. For the cathodoluminescence of silver clusters discussed below, the band around 2.5 eV from the substrate NiAl has to be considered and may mask faint plasmon resonances of the Ag clusters.

### 3.2. Silver nanoparticles grown at 300 K

From the previously published STM work [25] the general trend can be derived, that exceeding an Ag-exposure of a monolayer at room temperature the

island density remains at some  $10^{11} \text{ cm}^{-2}$ , whereas the average diameter of the particles increases with dosage. In comparison to other d-metals, silver forms the largest 3-dimensional aggregates on alumina films in comparison with the metals studied so far [26]. The STM topography of Fig. 4a and b show that according to our expectation silver clusters nucleate and grow at the line defects of the substrate. For the same sample, an area rich in step edges (displayed in (a)), leads to an island density of  $1 \times 10^{12} \text{ cm}^{-2}$  of the silver aggregates, whereas in a region free of steps as in (b), an apparently more extensive nucleation on domain boundaries prevails, leading to bigger clusters at a lower density of  $2 \times 10^{11} \text{ cm}^{-2}$ . The fact that in this case a distinct nucleation on the  $\text{Al}_2\text{O}_3$  point defects (density  $\sim 1 \times 10^{13} \text{ cm}^{-2}$ , not visible in the STM) [11] is not observed, can be explained by the low adhesion energy at these sites in comparison to thermal energy at 300 K. Concerning the optical spectra presented below, the variation of the average thickness (1–15 Å) affects mainly the size of silver nano particles as there is little change in the island density and in

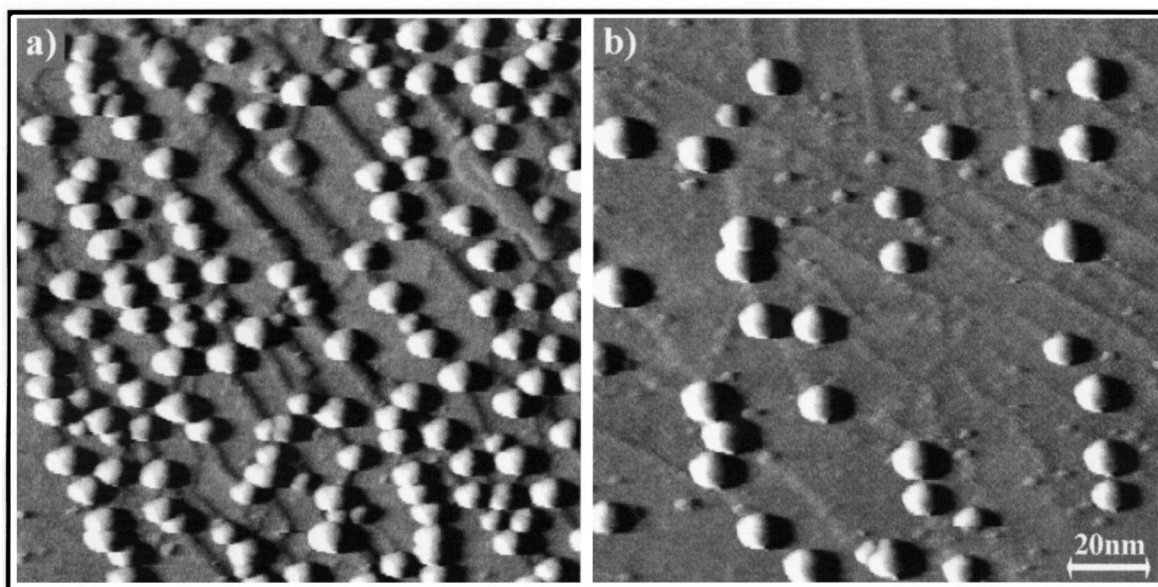


Fig. 4. STM images of Ag on an  $\text{Al}_2\text{O}_3$  film,  $138 \times 138 \text{ nm}^2$ ; (a) area rich in steps, (b) area free of steps.

aspect ratio (diameter/height) of 1.7, at least at 300 K.

Fig. 5 presents the cathodoluminescence spectra for different silver coverages prepared at 300 K. At 3.7 eV photon energy a distinct plasmon band appears, increasing in intensity with the amount of silver deposited, whereby no significant shift in peak position is observed. However, the broad NiAl luminescence seems to shift from 2.6 to 3.0 eV at highest silver deposition. For a free silver nanoparticle, the dipolar Mie resonance would be threefold degenerated. Upon deposition the resonance splits into a double degenerated component (1,1) at lower energy in comparison to the free cluster and a single mode (1,0) at higher energy. This is schematically shown in Fig. 6. The silver nanoparticles are oblate spheroids as we know from the STM study. We assign the Mie resonance at 3.7 eV in Fig. 5 to the (1,0) mode. This is strongly supported by the polarization measurement of the emitted photon intensity (Fig. 6), yielding a  $\sin^2$ -dependence with respect to the polarization angle  $\alpha$ . The excitation of the (2,0) quadrupole resonance (the resonance position is nearly identical with the (1,0) dipole mode for an oblate cluster) can be excluded, as the radiation should be elliptically polarized at the actual observa-

tion angle. Only at much higher electron energies of about 15 keV, Little et al. [30] could observe photon emission from a quadrupole plasmon excitation.

The (1,1) resonance is overlapping at photon energies of 2.5 to 3.0 eV with the NiAl luminescence band, a dependence on the polarization for this overlap band was not observed. Actually this is expected for the (1,1) plasmon (Fig. 6).

In order to deconvolute the resonance position and half width of the (1,0) mode, a superposition of the NiAl luminescence (as in Fig. 3) and a Lorentzian shape for the Mie resonance in the spectra (Fig. 5a) was assumed. According to this treatment, a slight shift of the (1,0) resonance energy of the supported silver cluster is observed with decreasing cluster size to higher values as indicated in Fig. 5b. The faint blue shift agrees with a  $1/R$ -dependence [27], that we observed for a wider range of particle size by the STM study on individual Ag clusters [12]. This trend is theoretically explained by Liebsch [28] to be due to the reduction of the s/d-electron coupling in silver at the cluster surface in comparison to the situation within the bulk. In this model the coupling is restricted to a core region at a distance  $D_M$  below the surface, in the surface region the spill out of the 5s-electrons will then contribute with a higher (un-

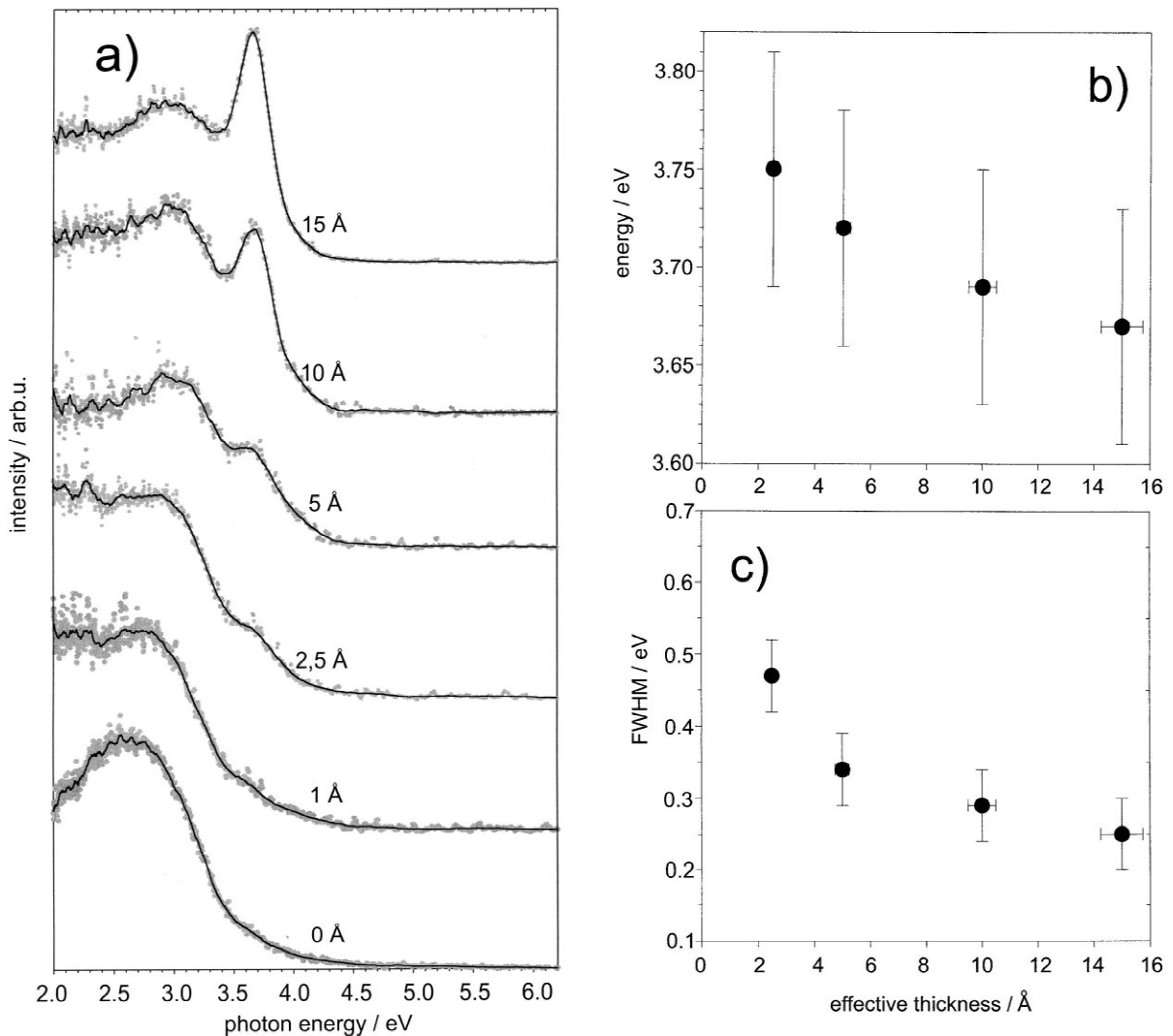


Fig. 5. (a) Spectra of Ag on  $\text{Al}_2\text{O}_3/\text{NiAl}$  at different silver coverages, (b) peak resonances depending on the coverage, (c) half width of the (1,0) resonance.

screened) plasma frequency. Such an effect becomes more pronounced with decreasing particle radius and thus increases the weight of the surface contribution. Liebsch derived a relation for the Ag Mie resonance depending on the reciprocal particle radius  $1/R$ :

$$\omega(R) = \omega_\infty [1 - 0.5D_M(\omega_\infty/\omega_s)^2 \cdot R^{-1} + O(R^{-2})]$$

where  $\omega_\infty$  denotes the resonance of a large spherical particle (3.5 eV), and  $\omega_s$  the surface plasmon fre-

quency. For free Ag clusters (spherical) the observed  $1/R$ -dependence levels out at an effective diameter of 10 nm [5]. The corresponding resonance energy equals 3.5 eV, a value predicted from the relation  $\varepsilon_1(\omega) = -2$ . However, for the silver cluster supported by the alumina film we observe an asymptotic value of about 3.7 eV for the Mie (1,0) resonance at mean cluster diameter of  $\sim 10$  nm. The blueshift of 200 meV of the supported Ag cluster in comparison to the free cluster has to be influenced therefore by

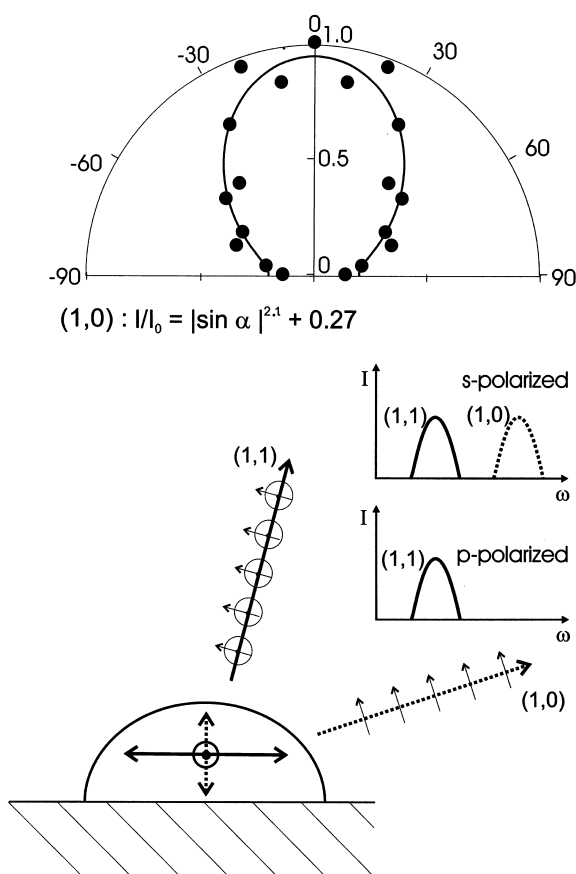


Fig. 6. Photon emission intensity of Ag cluster on  $\text{Al}_2\text{O}_3/\text{NiAl}$  for the (1,0) mode versus polarizing angle.

the different environment. In the literature [6] mainly the following reasons are discussed for the blue shift of the high energetic (1,0) mode:

- the electromagnetic coupling by surrounding silver particles,
- a nonspherical shape of the supported silver aggregates, and
- the electromagnetic coupling to the substrate.

Let us consider these possibilities one by one.

(a) The Mie resonance excitation of one cluster of the ensemble by the impinging electron induces an image dipole in the adjacent silver aggregates. The influence of this interaction can be estimated from STM experiments, whereby the light emission was detected from an isolated Ag cluster in comparison

with particles of same size but surrounded by many adjacent clusters. At a mean island density of some  $10^{11} \text{ cm}^{-2}$  the same resonance energy in both cases was observed within the experimental error. This indicates that the next neighbour interaction plays a minor role if a single cluster is excited. In the cathodoluminescence experiment clearly less than one electron arrives at the sample within the life time of the plasmon ( $<10 \text{ fs}$ ) at a current of  $5 \mu\text{A}$ , so simultaneous excitation of different clusters can be excluded. Only by multiple energy losses of the impacting electrons this could be achieved, but this is a rare process at an energy of  $50 \text{ eV}$  [29]. Thus we can transfer the STM results in this respect to the present experimental situation, where the excitation is induced by an electron beam from a source in a macroscopic distance. Consequently next neighbour coupling (a) should not significantly contribute to the observed blue shift. However for a 'long range excitation' by incoming light at a cluster density of typically some  $10^{11} \text{ cm}^{-2}$  a blue shift of the order of  $100 \text{ meV}$  is expected [9].

(b) The argument for a blue shift of the resonance energy is based on the splitting of the dipolar Mie resonance line into the (1,1) and (1,0) mode due to the breaking of spherical symmetry in the presence of a support ( $\text{Al}_2\text{O}_3/\text{NiAl}$ ). For free ellipsoids the shape dependence was modelled theoretically in the quasistatic approximation by Little et al. [30] and Kreibig et al. [6]. According to these calculations a blue shift of  $100$  to  $200 \text{ meV}$  is expected for the (1,0) mode of oblate Ag clusters with an aspect ratio of  $1.7$ , derived from our STM measurements. Including the image dipole interaction of the support and the adjacent clusters, Yamaguchi et al. [32,33] and Little et al. [30] modelled the resonance energy dependence on the axial ratio of the spheroids for the (1,0) mode; it is only negligibly different compared to the free cluster, whereas the low energetic (1,1) mode shows a noticeable redshift increasing with  $\epsilon$  of the dielectric support [31]. A calculation by Wenzel et al. based on Ref. [34] provides essentially the same result with the deviation that the dielectric support yields already, in the limit of a sphere, a splitting into two modes. This means the shape influence (b) and the electromagnetic coupling to the substrate (c) cannot be discussed separately. For example a blueshift of  $200 \text{ meV}$  is given by the calculation of

Hövel et al. [31] for silver spheroids on quartz glass for an aspect ratio of 1.7, but the coupling to the dielectric partly compensates this shift to a resonance position of 3.55 eV. This counter balancing effect as observed for a dielectric support seems to be ineffective for an ultrathin  $\text{Al}_2\text{O}_3$  film on a NiAl substrate. In general, a red shift of the Mie resonance of an Ag particle is expected in a dielectric environment [6]. This results from in-phase coupling of the image dipole in the substrate with the plasmon and thus weakens the restoring force acting on the electrons. An underlying metal could change the coupling due to the different phase relation of the image dipole. Using graphite as a support, Grimaud et al. [35] observe for an Ag cluster deposit with high density a plasmon resonance at 3.85 eV exhibiting a very faint dispersion. The blue shift of 150 meV with respect to bulk silver (3.7 eV) is attributed to the low thickness of the film and the coupling to the graphite support. Although the authors state an Ag cluster size of 10 nm in the dense film, the electromagnetic coupling between the nanoparticles is not considered (a blue shift is expected from Ref. [9]). Similar blue shifts in granular films are observed in an EELS study by Moresco et al. [36] using silicon as a support. It is very likely that those shifts are caused by interparticle coupling and not by the support. For that reason they are not directly relevant for an interpretation of the present data.

In a simple approach we estimate the interaction with the NiAl support. Considering the damping effect, we determine from the polarization term  $P$ :

$$P(i\omega t - i\gamma) = \varepsilon_0[\varepsilon(\omega) - 1] \cdot E_0 e^{i\omega t}$$

a phase shift  $\gamma$  of  $80^\circ$  for the image dipole by inserting the value of the complex permittivity for NiAl around the resonance frequency. From this estimation a pronounced weakening of the restoring power for the Mie oscillator in contrast to a dielectric cannot be expected because the interacting dipoles are out of phase. Although this reasoning is only of qualitative nature we interpret the observed blue shift of the (1,0) resonance being induced by: (i) the oblate shape of the silver cluster, and (ii) the reduced interaction between the (1,0) plasmon and the image dipole in the NiAl. The oxide film as the actual support (thinner than the cluster diameter) does not contribute to the electromagnetic coupling.

Another important parameter of describing the observed plasmon resonance is the full width at half maximum (FWHM). By photon emission measurements on individual Ag clusters with the STM, we have evaluated the intrinsic width of 150 meV for a large silver particle on  $\text{Al}_2\text{O}_3/\text{NiAl}$  [13]. For ensemble measurements as presented in this contribution, a higher value of 250 meV is measured for a 10 nm particle. The inhomogeneous broadening of the plasmon band is expected because of averaging over the size and shape distribution on the surface. Nevertheless with decreasing effective thickness of the silver layer an increase of the FWHM to 480 meV is observed.

### 3.3. Silver nanoparticles grown at 90 K

For kinetic reasons the preparation of Ag clusters at a probe temperature of 90 K leads to smaller cluster sizes, a more oblate shape and higher particle densities [26], as compared to a deposition at room temperature. However, the investigation of the actual size distribution of the clusters was not possible with the STM at 90 K. The predominance of small clusters agrees with the observed high value for the (1,0) mode at around 3.9 eV in Fig. 7a. The position of the Mie plasmon shifts only little when the average thickness of the deposited silver is increased from 5 to 12.5 Å (Fig. 7b), presumably because of a mutual cancellation of size and shape effects during cluster growth. Again the low energetic (1,1) mode is partly overlapping with the emission from the NiAl support (Fig. 7a).

By annealing these samples to 900 K for 20 s, the (1,0) resonance position shifts to a value of  $\sim 3.7$  eV, similar to the one observed on the 300 K samples. Qualitatively this can be interpreted as a consequence of growing particle size and decreasing aspect ratio of the silver cluster, but from the energy shift alone the two effects cannot be distinguished. Using the photon emission around 3 eV in Fig. 7a as a guide line for the (1,1) plasmon mode, the observed shift to higher resonance energies as well as the increase in intensity of this mode after heat treatment indicates a growth and a transition of the silver cluster to a more spherical shape. In order to get more detailed information on the position and the FWHM of the (1,0) resonance, the annealing pro-

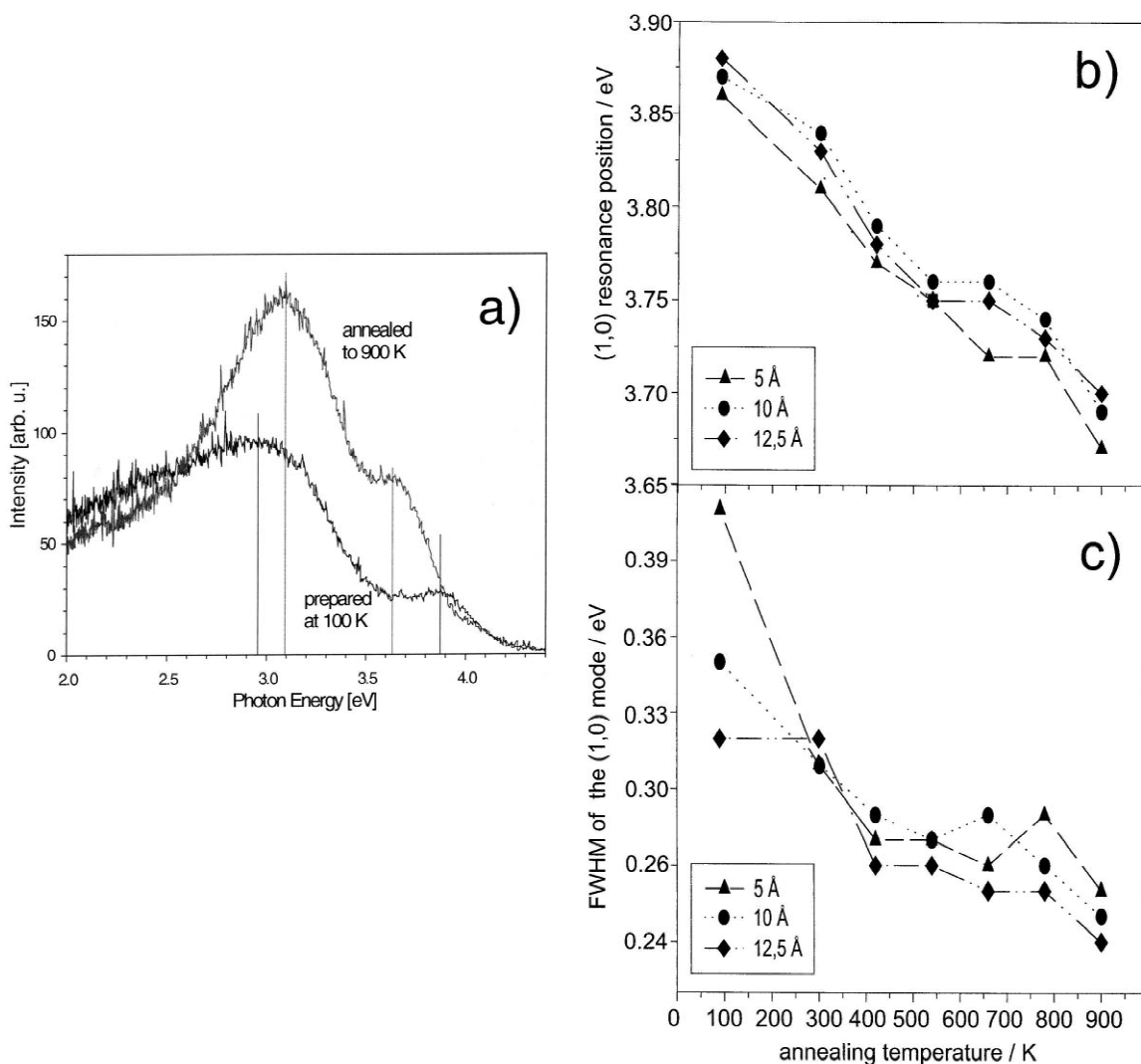


Fig. 7. Effect of annealing (a) silver deposited on  $\text{Al}_2\text{O}_3/\text{NiAl}$  at 90 K and annealed at 900 K for 20 s, (b) shift of the (1,0) resonance energy with annealing temperature, (c) half width of the (1,0) resonance versus annealing temperature.

cedure was performed stepwise (Fig. 7b and c) in addition. Even after annealing at room temperature for 20 s, the blueshift, narrowing and intensity increase of the (1,0) resonance line is observed, reflecting the growth and rounding of the silver nanoparticles. The corresponding redshift of the (1,1) mode (not shown) supports this interpretation. Annealing temperatures of 100 K for a sample with silver deposited at 30 K showed no significant

changes in optical spectra, which indicates that Ag/Ag-selfdiffusion starts at a temperature above 100 K

The break in the red shift with increasing annealing temperature (Fig. 7b) above 500 K seems to mark a change from coalescence to Ostwald ripening growth of the Ag particles [37,38] above 600 K, whereas the shape does not change any more as the (1,1) resonance position becomes stable then.

Similar to the resonance position the width in Fig.

7b displays an even more pronounced plateau above 400 K annealing temperature indicating a saturation of the growth process according to the  $1/R$  relationship [2,10]. At still higher temperatures of 800 K the width of the Mie resonance will further decrease due to a particle growth by Ostwald ripening. It is striking that after the highest annealing temperature applied, a decrease of the luminescence intensity is observed. This is interpreted as a loss of silver nanoparticles on the oxide film, possible by a penetration of silver through the film, as observed e.g. for Pd clusters [26]. Another process is the starting evaporation of silver at 820 K as measured by thermal desorption of silver from  $\text{Al}_2\text{O}_3$  films by van Campen et al. [39]. In all three processes the disappearance of smaller clusters is favoured kinetically, with the effect of shifting the mean cluster size to higher values.

#### 4. Summary

In this paper, we have reported on cathodoluminescence experiments on Ag clusters grown on an ultrathin alumina film on NiAl (110) by Ag deposition from an electron beam evaporator. The clusters were prepared at different temperatures and Ag coverages leading to a mean cluster size between 2 and 12 nm, as deduced from STM-measurements. The nucleation is preferred at defect sites, such as steps and domain boundaries.

The impact of electrons with typically 50 eV energy excites dipolar Mie plasmons in the supported silver clusters. The analysis of the polarization of the light, emitted after radiating decay of the Mie plasmons, allows an assignment to the parallel (1,1) and perpendicular (1,0) mode of the plasmon. The (1,1) resonance is masked partly by the light emission at about 2.6 eV from the underlying NiAl. The high resonance energy of 3.7 eV of the (1,0) mode at 10 nm cluster size is caused by the oblate shape with an aspect ratio of about 2 for the silver spheroid. This oblate cluster shape is supported by the position of the (1,1) resonance. The coupling to next neighbor clusters is of minor importance at an actual island density of some  $10^{-11} \text{ cm}^{-2}$ . The interaction with the underlying NiAl can be neglected, as the induced image dipole according to the dielectric

function of this alloy dynamically yields a phase shift of about  $90^\circ$  and does not couple constructively with the (1,0) plasmon of the silver particle.

In annealing experiments the silver aggregates start to grow in size above temperatures of 100 K because of the low adhesion energy to aluminium oxide. The high mobility of silver on silver also causes more rounded cluster shapes. The thermodynamically favored shape of the aggregates as realized at high temperatures has still an oblate character. At very high temperatures above 800 K the loss of silver particles was deduced from the optical spectra.

#### Acknowledgements

We are grateful for the financial support of the Deutsche Forschungsgemeinschaft, of the Fond der Chemischen Industrie, and of the NEDO International Joint research Grant on Photon and Electron Controlled Surface Processes. Further we thank J. Jupille, R. Lazzari, and N. Ernst for fruitful discussion.

#### References

- [1] G. Mie, *Ann. Phys.* 25 (1908) 377.
- [2] U. Kreibig, M. Vollmer, *Optical Properties of Metal Clusters*, Springer, Berlin, 1995.
- [3] M.I. Stockman, *Phys. Rev. Lett.* 84 (2000) 1011.
- [4] R. Borek, K.-J. Berg, *Glass Sci. Techn.* 71 (1998) 352.
- [5] H. Hövel, S. Fritz, A. Hilger, U. Kreibig, M. Vollmer, *Phys. Rev. B* 48 (1993) 18178.
- [6] U. Kreibig, *J. Phys. F: Metal Phys.* 4 (1974) 999.
- [7] D. Martin, J. Jupille, Y. Borenstein, *Surf. Sci.* 402 (1998) 433;  
T. Wenzel, J. Bosbach, F. Stietz, F. Träger, *Surf. Sci.* 432 (1999) 257.
- [8] U. Kreibig, L. Genzel, *Surf. Sci.* 156 (1985) 678.
- [9] F. Stietz, F. Träger, *Phil. Mag. B* 79 (1999) 1281.
- [10] C.R. Henry, *Surf. Sci. Rep.* 31 (1998) 231.
- [11] H.J. Freund, M. Bäumer, H. Kuhlenbeck, *Adv. Catal.* 45 (2000) 333.
- [12] N. Nilius, N. Ernst, H.-J. Freund, *Phys. Rev. Lett.* 84 (2000) 3994.
- [13] P. Dumas, S. Strykh, I. Marennko, F. Salvan, *Europhys. Lett.* 40 (1997) 447.
- [14] R.M. Jaeger, H. Kuhlenbeck, H.-J. Freund, M. Wuttig, W. Hoffmann, R. Francy, H. Ibach, *Surf. Sci.* 259 (1991) 235.

- [15] J. Libuda, F. Winkelmann, M. Bäumer, H.-J. Freund, Th. Bertrams, H. Neddermeyer, K. Müller, *Surf. Sci.* 318 (1994) 61.
- [16] C.T. Campbell, *Surf. Sci. Rep.* 27 (1997) 1.
- [17] M. Adelt, R. Körber, W. Drachsel, H.-J. Freund, *Rev. Sci. Instrum.* 70 (1999) 3886.
- [18] H.P. Kallmann, G.M. Spruch (Eds.), *Luminescence of Organic and Inorganic Materials*, Wiley, New York, 1962.
- [19] N. Nilius, N. Ernst, P. Johansen, H.-J. Freund, *Phys. Rev. B* 61 (2000) 12682.
- [20] E.D. Palik (Ed.), *Handbook of Optical Constants of Solids*, Academic Press, Orlando, 1985.
- [21] I. Frank, V. Ginsburg, *J. Phys.* 9 (1945) 359.
- [22] A. Kramers, *Phil. Mag.* 46 (1923) 836.
- [23] J.J. Rechten, C.R. Kannewurf, J.O. Brittain, *J. Appl. Phys.* 38 (1967) 3045;  
H. Jacobi, R. Stahl, *Z. Met.* 60 (1969) 106;  
H. Jacobi, R. Stahl, *J. Phys. Chem. Solids* 34 (1973) 1737;  
D. Knab, C. Koenig, *J. Phys. Condens. Matter* 2 (1990) 465;  
K.J. Kim, B.N. Harmon, D.W. Lynch, *Phys. Rev. B* 43 (1991) 1948.
- [24] D.J. Peterman, R. Rosei, D.W. Lynch, V.L. Moruzzi, *Phys. Rev. B* 21 (1980) 5505.
- [25] H.-J. Freund, B. Dillmann, D. Ehrlich, M. Haßel, R.M. Jaeger, H. Kuhlenbeck, C.A. Ventrice Jr., F. Winkelmann, S. Wohlrab, C. Xu, Th. Bertrams, A. Brodde, H. Neddermeyer, *J. Mol. Catal.* 82 (1993) 143.
- [26] M. Bäumer, H.-J. Freund, *Prog. Surf. Sci.* 61 (1999) 127.
- [27] U. Heiz, A. Vayloyan, E. Schumacher, *Rev. Sci. Instrum.* 68 (1997) 3718.
- [28] A. Liebsch, *Phys. Rev. B* 48 (1993) 11317.
- [29] F. Moresco, M. Rocca, V. Zielasek, T. Hildebrandt, M. Henzler, *Surf. Sci.* 389 (1997) 1.
- [30] J.W. Little, T.A. Callcott, T.L. Ferrell, E.T. Arakawa, *Phys. Rev. B* 29 (1984) 1606.
- [31] H. Hövel, A. Hilger, I. Nusch, U. Kreibitz, *Z. Phys. D* 42 (1997) 203.
- [32] T. Yamaguchi, S. Yoshida, A. Kinbara, *Thin Solid Films* 21 (1973) 173.
- [33] T. Yamaguchi, M. Ogawa, H. Takahashi, N. Saito, E. Anno, *Surf. Sci.* 129 (1983) 232.
- [34] T. Wenzel, J. Bosbach, F. Stietz, F. Träger, *Surf. Sci.* 432 (1999) 257.
- [35] C.M. Grimaud, L. Siller, M. Andersson, R.E. Palmer, *Phys. Rev. B* 59 (1999) 9874.
- [36] F. Moresco, M. Rocca, T. Hildebrandt, M. Henzler, *Phys. Rev. Lett.* (1999) 2238.
- [37] I.M. Lifshitz, V.V. Slezov, *J. Phys. Chem. Solids* 19 (1961) 35.
- [38] C. Wagner, *Ber. Bunsenges. Phys. Chem.* 65 (1961) 581.
- [39] D.G. van Campen, J. Hrbeck, *J. Phys. Chem.* 99 (1995) 16389.